PROCEEDINGS B

royalsocietypublishing.org/journal/rspb

Research



Cite this article: Fenwick AJ, Lin DC, Tanner BCW. 2021 Myosin cross-bridge kinetics slow at longer muscle lengths during isometric contractions in intact soleus from mice. *Proc. R. Soc. B* **288**: 20202895. https://doi.org/10.1098/rspb.2020.2895

Received: 22 January 2021 Accepted: 22 April 2021

Subject Category:

Morphology and biomechanics

Subject Areas:

biomechanics, biophysics, cellular biology

Keywords:

myosin cross-bridges intact muscle

Author for correspondence:

Bertrand C. W. Tanner

e-mail: bertrand.tanner@wsu.edu

Myosin cross-bridge kinetics slow at longer muscle lengths during isometric contractions in intact soleus from mice

Axel J. Fenwick^{1,2}, David C. Lin^{1,2,3} and Bertrand C. W. Tanner^{1,2}

D AJF, 0000-0002-8296-537X; DCL, 0000-0003-4492-0944; BCWT, 0000-0003-1711-8526

Muscle contraction results from force-generating cross-bridge interactions between myosin and actin. Cross-bridge cycling kinetics underlie fundamental contractile properties, such as active force production and energy utilization. Factors that influence cross-bridge kinetics at the molecular level propagate through the sarcomeres, cells and tissue to modulate wholemuscle function. Conversely, movement and changes in the muscle length can influence cross-bridge kinetics on the molecular level. Reduced, singlemolecule and single-fibre experiments have shown that increasing the strain on cross-bridges may slow their cycling rate and prolong their attachment duration. However, whether these strain-dependent cycling mechanisms persist in the intact muscle tissue, which encompasses more complex organization and passive elements, remains unclear. To investigate this multi-scale relationship, we adapted traditional step-stretch protocols for use with mouse soleus muscle during isometric tetanic contractions, enabling novel estimates of length-dependent cross-bridge kinetics in the intact skeletal muscle. Compared to rates at the optimal muscle length (L_0) , we found that cross-bridge detachment rates increased by approximately 20% at 90% of Lo (shorter) and decreased by approximately 20% at 110% of $L_{\rm o}$ (longer). These data indicate that cross-bridge kinetics vary with whole-muscle length during intact, isometric contraction, which could intrinsically modulate force generation and energetics, and suggests a multi-scale feedback pathway between whole-muscle function and cross-bridge activity.

1. Introduction

Skeletal and cardiac muscles have robust length-dependent properties that influence active force generation. These have been primarily investigated at the single fibre and myofibril scale, through which studies have elucidated how filament overlap, lattice spacing, calcium sensitivity and other properties can change with the length of a muscle fibre to alter force [1-7]. Other studies have shown that actin-myosin cross-bridge kinetics slow at longer sarcomere lengths in skinned (permeabilized) skeletal and cardiac muscle fibres [8,9], a mechanism that may contribute to the Fenn effect and underlie contractile efficiency of cardiac and skeletal muscle during physiological movements [10-12]. However, the effects of varied muscle length on cross-bridge kinetics in an intact skeletal muscle preparation remain undefined. This is an important point of study because the whole muscle is connected to the tendon and other connective tissue, which influence the length changes in the muscle and consequently its force generation. We hypothesize that the strain-dependent myosin activity extends from the molecular and cellular levels to influence contractile properties at the intact muscle tissue level. Support of this hypothesis implies that length-dependent myosin activity impacts muscle function under physiological conditions, not just under reduced experimental conditions.

¹Department of Integrative Physiology and Neuroscience, ²Washington Center for Muscle Biology, and ³The Gene and Linda Voiland School of Chemical Engineering and Bioengineering, Washington State University, Pullman, WA 99164, USA

Sinusoidal length perturbations across a range of frequencies have helped described that the muscle stress response arises from the cross-bridge activity and passive elements of the muscle [13]. This approach has been further developed to describe characteristics of muscle work production (i.e. cross-bridge recruitment rates) and work absorption (i.e. cross-bridge detachment rates) for a contracting muscle [13-15]. Frequency-dependent length perturbation analysis methods are difficult to apply to intact muscle preparations due to the relatively long duration that a muscle must maintain steady tetanic contraction (to resolve the low-frequency responses). An alternative method is used to apply a small step-stretch perturbation to the muscle and to measure the time-dependent force response [16-20]. In this study, we applied step-stretches of 1% change in length (ΔL) to intact, isometric, tetanically contracting mouse soleus muscle-tendon unit (MTU). The time-dependent stress-strain response was fitted to a mathematical model [15] that is analogous to the frequency-dependent model we used to estimate cross-bridge kinetics in permeabilized muscle fibres [8,9]. This model consists of: (i) an exponential process describing the rapid decay in stress following the stretch, used to estimate cross-bridge detachment rate (akin to phase 2 of Huxley and Simmons [17]); (ii) an exponential process describing the slower redevelopment of stress following the stretch, used to estimate cross-bridge attachment rate (akin to phase 3 [17]); and (iii) a fractional derivative representing the viscoelastic stress response following the stretch, due to passive elements in the muscle-tendon unit responding to a new length (or loading regime).

We initially tested our ability to estimate cross-bridge kinetics using this model, showing the expected temperature-dependent acceleration of cross-bridge recruitment and detachment rates from 17°C to 27°C. Next, we proceeded to estimate length-dependent effects on cross-bridge recruitment and detachment kinetics at optimal muscle length ($L_{\rm o}$), at 0.9 $L_{\rm o}$ and at 1.1 $L_{\rm o}$ to characterize the effect of the MTU length on cross-bridge kinetics. Our data provide further evidence that the muscle length directly influences cross-bridge kinetics in a contracting muscle, which implies that a length-dependent mechanism at the cross-bridge level modulates intact muscle efficiency.

2. Materials and methods

(a) Animal models

Downloaded from https://royalsocietypublishing.org/ on 12 May 202

All procedures were approved by the Institutional Animal Care and Use Committee at Washington State University and complied with the *Guide for the Use and Care of Laboratory Animals* published by the National Institutes of Health. Ten male C57BL/6 mice (7 weeks old; Simonsen Laboratories) were anaesthetized by isoflurane inhalation (3% volume in 95% O₂–5% CO₂ flowing at 2 l min⁻¹). A soleus MTU was removed (one per mouse), preserving as much of the proximal and distal tendons as possible, and immediately placed in the experimental chamber containing oxygenated Ringer's solution.

(b) Tetanic step procedure

Soleus muscles were suspended in a temperature-controlled (17°C or 27°C), oxygenated chamber (95% O_2 –5% CO_2) with the distal tendon (and a small piece of the calcaneus) sutured onto a force transducer (Aurora Scientific 407A; response time of 2 ms for 1%–99% of the motor's length range), and the proximal tendon was sutured onto a length controller (Aurora

Scientific 305C). The length of suture needed to securely attach the MTU was kept to a minimum, and the MTU was tied directly to the metal hook on the motor or force transducer, both of which helped reduce added compliance between the MTU preparation and equipment. Muscles were equilibrated with Ringer's solution (154 mM NaCl, 5.6 mM KCl, 1 mM MgCl₂, 2.2 mM CaCl₂, 10 mM glucose, 20 mM HEPES, pH 7.4 [21]) for 5 min. Muscles were field stimulated (Aurora scientific 701C) via parallel electrode plates along the length of the chamber at 20 V (0.2 ms pulse width) and 100 Hz to measure the maximum isometric tetanic force (figures 1 and 2). Muscle length was set by changing the motor position in relation to the force transducer. Optimal MTU length (Lo) was determined by tetanically stimulating the muscle at multiple lengths (minimum of 5 lengths, each followed by at least 3 min rest to minimize fatigue). Maximal tetanic stress values were determined by averaging the stress versus time data over the final 20 ms of the stimulation period, before the end of electrical excitation. L_o was then defined as the length that generated maximum active force (total force minus passive force) along the force-length curve (figure 2). Once L_0 was established, the MTU was set to one of the three lengths: Lo, 90% of Lo or 110% of Lo. Tetanic contraction was then induced in the muscle for 2 s, with a 1% step-stretch increase in the MTU length at each of the three lengths tested, applied at 1s and held for the remainder of the activation period (figure 3). We used constant strain for the step amplitude rather than the constant absolute length to normalize and compare muscles of different sizes. This procedure was then repeated for the remaining two lengths and then again for all three lengths at the other test temperature. The order of the MTU length and the temperature of the chamber (17°C or 27°C) were randomized for each experiment to reduce the possible influence of fatigue.

After mechanical experiments were completed, muscle and tendons were separated, measured and weighed to estimate the physiological cross-sectional area (CSA [23]):

$$CSA = \frac{m \times \cos(\theta)}{(L_f \times \rho)},$$
(2.1)

where m is muscle mass, θ is pennation angle (= 8.5° for soleus muscle [24]), L_f is fibre length calculated from the fibre-to-muscle length ratio (= 0.71 for soleus muscle [25]) and ρ is the muscle density (= 1.06 mg mm⁻³ [26]). The average CSA of the soleus muscle was 1.01 ± 0.07 mm². Force was then divided by the CSA to calculate stress.

(c) Step length perturbation analysis

The striated muscle responds to a sudden length increase with a force response that has classically described the following 'phases' [17,19,20,27]. In phase 1, the force rises instantaneously as attached cross-bridges and elastic elements are strained (figure 3, σ_0 to σ_1). In phase 2, the force decays as cross-bridges detach in a synchronized manner (figure 3, σ_1 to σ_2). Next, the force rises in phase 3 due to cross-bridge recruitment, the force response plateaus at an elevated level (i.e. $\sigma_{\text{final}} > \sigma_0$) due to passive properties of the muscle at the new, longer muscle length (i.e. stretching tendon, connective tissue, titin and collagen). These phases are a time-domain representation of the same processes observed in the frequency domain via sinusoidal length perturbation analysis, both of which describe enzymatic and mechanical properties of the muscle [13,15,28]. The time-dependent viscoelastic stiffness, or modulus response, $Y(t) = \sigma(t)/\varepsilon(t)$, arises from the time-dependent stress response ($\sigma(t)$) to the muscle strain ($\varepsilon(t)$). The step-function change in the muscle length can be characterized by equation (2.2), as described by Palmer et al. [15]:

$$Y(t) = At^{-k} - Be^{-2\pi bt} + Ce^{-2\pi ct},$$
(2.2)

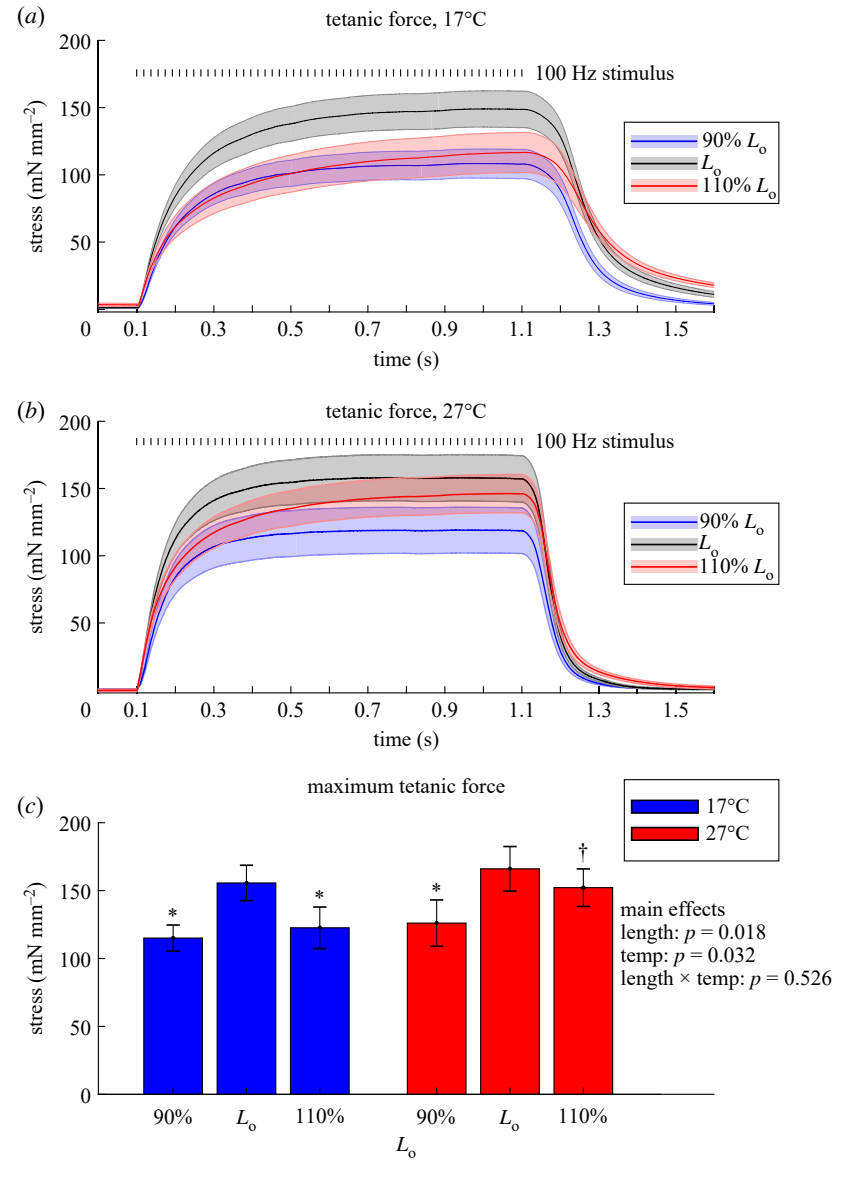


Figure 1. Tetanic stress of electrically stimulated mouse soleus muscle. (a) Average muscle stress (solid lines) is plotted against time for three muscle lengths: optimal length (L_0) and $\pm 10\%$ MTU length of L_0 (shaded regions represent SEM for each length). Tetanic contractions were elicited for 1 s via 20 mV stimuli at 100 Hz, with example data shown solely for 17°C. (b) Maximal stress of tetanically stimulated muscle at three muscle lengths for 17°C and 27°C. (c) Maximal stress was determined as average stress over the final 20 ms before the end of electrical excitation. Asterisks denote differences from the measured value at L_0 within a temperature (p < 0.05), and the dagger denotes differences between temperatures for the same muscle length. n = 10 muscles.

The molecular, cellular and tissue characteristics described by equation (2.2) represent a model appropriately describing Y(t) for the measured stress–strain response between σ_1 and σ_{final} with the initial time-point occurring at the onset of the strain stimulus (i.e. t=0 at t_0 for σ_0 ; figure 3). Parameter A represents the combined mechanical stress of the muscle and tendon, while parameter k describes the viscoelasticity of the passive elements; a k value of 0 represents a purely elastic response and a k value of 1 represents a purely viscous response [29]. The B and C processes are analogous to the work-producing and work-absorbing process described earlier during phase 3 for cross-bridge recruitment and phase 2 for cross-bridge detachment [14,15,30,31]. B and C represent the mechanical stress from the bound cross-bridges, and $2\pi b$ and $2\pi c$ reflect cross-bridge recruitment rate and detachment rate, respectively.

To best emulate physiological conditions, both the proximal and distal tendons of the muscle preparations were left intact. However, the tendons add an additional in-series elastic element that should be considered when applying the small step analysis to ensure that the muscle (and not tendon) is

primarily experiencing the perturbation. We calculated the tendon area and the length to provide an estimate of tendon stiffness (K_T) [32]:

$$K_T = \frac{EA_T}{l_T},\tag{2.3}$$

where E is the elastic modulus (reported to be approximately 62 N mm⁻² for mouse soleus tendon [33]), A_T is the calculated tendon area (0.59 mm²) and l_T is the measured tendon length (7.2 ± 0.18 mm) at L_o . Thus, we roughly estimate K_T = 5.1 N mm⁻¹. Average MTU L_o was 15.22 ± 0.37 mm, so a 1% step-stretch stretched the MTU 0.15 mm. This stretch produced an average increase in the force of 0.16 N (phase 1) for MTU stiffness (K_{MTU}) of 1.05 N mm⁻¹. Solving for muscle stiffness (K_M):

$$K_{MTU} = \frac{K_M K_T}{K_M + K_T},\tag{2.4}$$

we estimate average $K_m = 1.3 \text{ N mm}^{-1}$. These values suggest that tendon stiffness is approximately four times greater than muscle

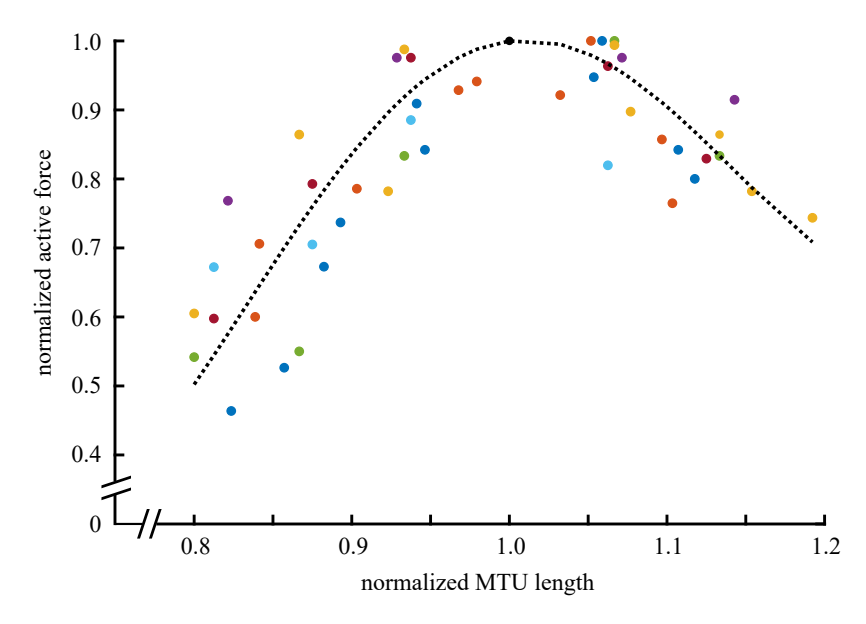


Figure 2. Composite force—length relationship from 10 MTUs. Each MTU was stimulated at 20 V and 100 Hz of 0.2 ms pulse width for 1 s. Each colour represents a single MTU from a single mouse. Force measurements were made at 5–7 lengths from each muscle. Dashed line represents a fourth-order polynomial fit to the composite data [22].

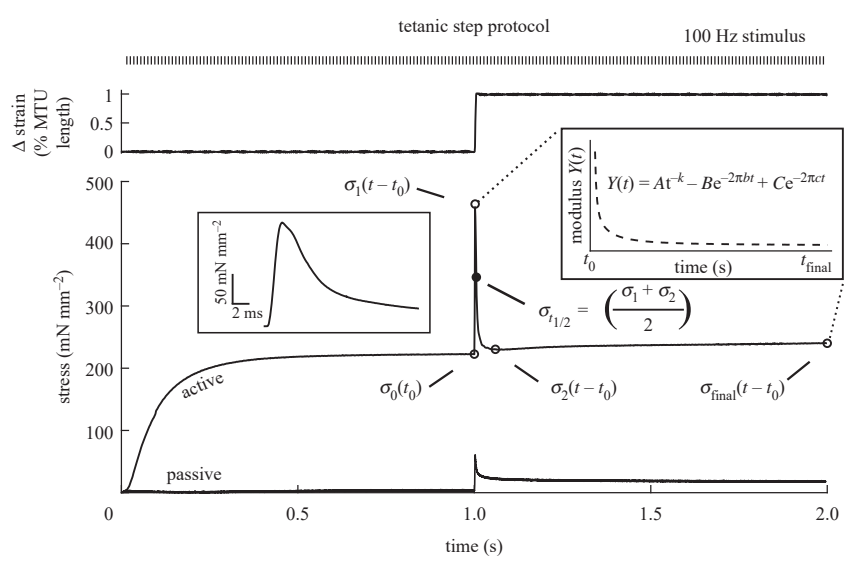


Figure 3. Protocol for step-stretch and modulus response of an example muscle during tetanic muscle contraction. Upper trace: motor position is plotted against time, where the MTU was stretched 1% of the total MTU length and then held at that longer length to enable measurement of the muscle stress—strain relationship. Middle trace: active muscle stress (σ) was plotted against time; muscle stress increased toward maximal isometric stress as the muscle was stimulated, and then stress briefly spiked with the step-stretch change (i.e. the strain stimulus initiated at time $t = t_0$), followed by stress decaying towards a new steady-state value at the longer MTU length. The open circle at σ_0 denotes muscle stress at time $t = t_0$, representing the tetanic stress value when the step-stretch was applied. Maximal stress is denoted by σ_1 (open circle), and the nadir of the subsequent stress response is denoted by σ_2 (open circle). The closed circle at $\sigma_{t1/2}$ represents the timepoint and stress value 50% of the way between σ_1 and σ_2 . Left inset: enhanced time scale of the rise and fall phase surrounding the step-stretch. Right inset: the modulus response as function of time (Y(t) = stress (t)/strain (t)), decaying from the maximum value at σ_1 , was fitted to equation (2.2) to estimate kinetic parameters. Bottom trace: passive muscle stress plotted against the same time scale with a step-stretch protocol, but in the absence of electrical stimulation.

stiffness, and thus we assume that for a given length increase, the muscle fibres experienced the majority of the length change from the step-stretch, with minimal work done on the tendon.

(d) Statistical analysis

Downloaded from https://royalsocietypublishing.org/ on 12 May 202

All data are listed as mean ± s.e.m. Sequential quadratic programming methods in Matlab (v. 9.4.0, The Mathworks) were used for constrained non-linear least-square fitting of equation (2.2) to moduli data for each individual muscle. Statistical analysis of experimental data was performed in SPSS (IBM Statistics), implementing linear mixed models with muscle length and temperature as repeated measures where appropriate. This approach matches data from the same muscle to provide more statistical power than a one-way analysis of variance. First-order autoregression was assumed for the covariance structure, and post hoc analyses were performed using least-significant difference corrections where appropriate. Statistical significance is reported at p < 0.05.

3. Results

Muscles were field stimulated to induce contraction and exhibited slow force rise and decay times characteristic of slow-twitch muscle (figure 1). We found the $L_{\rm o}$ of each MTU by sampling the force–length profile during tetanic contraction (figure 2). The shape of the resulting force–length was similar to in~situ MTU experiments with the medial gastrocnemius muscle, with a clearly defined $L_{\rm o}$ [34]. We measured stress values at $L_{\rm o}$ as well as $\pm 10\%~L_{\rm o}$ at 17°C and 27°C (table 1). Soleus muscles at 10% shorter MTU length generated on average approximately 25% less maximal tension, without a temperature dependence, while 10% greater MTU length generated on average 22% less tension at 17°C and 8% less at 27°C (figure 1).

Next, we induced tetanic contraction with the same stimulus used for the isometric measurements and applied a stepstretch increase of 1% ΔL after isometric force reached a steady state. As shown in the sample trace (figure 3), isometric tetanic stress increased towards a steady-state level during the initial half (= 1 s) of the stimulation period. When the muscle was stretched (at time = t_0), stress (σ) increased towards a maximal value (σ_1) , following which stress decayed towards a minimum value (σ_2). The stress then increased slightly to reach a new isometric force level (σ_{final}) that was greater than the initial isometric stress value (σ_0). The average moduli– time responses at L_o for 17°C and 27°C (figure 4) illustrated faster dynamic responses at the higher temperature, as would be expected for faster cross-bridge kinetics at the higher temperature. For example, $t_{1/2}$ (= the time required to reach the midpoint from σ_1 to σ_2) was 70% faster at 27°C $(4.9 \pm 0.4 \text{ ms})$ than 17°C $(8.4 \pm 0.8 \text{ ms}; \text{ table 1})$.

We also measured the effect of initial muscle length on the stress response to a 1% step-stretch, at both temperatures. Average moduli responses are shown for 17°C (figure 5a) and 27°C (figure 5b; note that the traces for L_0 shown in figure 5 are the identical traces shown in figure 4). For both temperatures, muscles exhibited significantly slower dynamics for the moduli-time responses as the muscle length increased. For reference, $t_{1/2}$ values were approximately 65% shorter at 90% MTU length versus values at $L_{\rm o}$ and approximately 15% longer at 110% MTU length versus values at L_o at 17°C (figure 5a and table 1). Consistently, $t_{1/2}$ values were approximately 25% shorter at 90% MTU length versus values at $L_{\rm o}$ and approximately 15% longer at 110% MTU length versus values at L_0 at 27°C (figure 5b) and table 1). Following the step-stretch, steady-state force (σ_{final}) was consistently higher compared to initial tension values before the step-stretch (σ_0 ; table 1), which may represent an estimate of the average force enhancement following a 1% stretch.

The mathematical model (equation (2.2)) that was fitted to each moduli–time response describes viscoelastic dynamics of the passive elements (A term) and the active elements (B and C processes). Average parameter values for moduli fits to equation (2.2) are listed in table 1 and shown in figure 6. A values were significantly greater at both 90% and 110% MTU lengths compared to $L_{\rm o}$ (figure 6a), and A values decreased at the higher temperature for all MTU lengths. Conversely, k values were smaller at both shorter and longer MTU lengths compared to $L_{\rm o}$ for both temperatures, indicating a more elastic characteristic of the MTU at $L_{\rm o}$ compared to non-optimal lengths (figure 6b).

Table 1. Parameter fits to equation (2.2) and other metrics associated with the stress response to the 1% MTU step-stretch (mean \pm s.e.). r^2 is the correlation coefficient for fits to equation (2.2), σ_0 is the initial active stress prior to the step stretch and $t_{1/2}$ is the time for the step response to decay by half.

		equation (2.2	equation (2.2) parameters								
temp (°C)	°7 %	A (kPa)	k	B (kPa)	$2\pi b \ (s^{-1})$	C (kPa)	$2\pi c (s^{-1})$ r^2	r ²	t _{1/2} (ms)	σ_0 (mN mm ⁻²)	$(\sigma_{final} - \sigma_0)/\sigma_0$ (%)
17℃	%06	2076 ± 196	0.35 ± 0.02	2782 ± 164	3.05 ± 0.10	15216 ± 2112	246 ± 21	0.9988 ± 0.0003	5.1 ± 0.6	132 ± 9	12.79
	100%	1481 ± 168	0.48 ± 0.02	1169 ± 178	2.20 ± 0.11	8572 ± 1453	207 ± 19	0.9994 ± 0.0002	8.4 ± 0.8	170 ± 11	7.85
	110%	2101 ± 294	0.38 ± 0.03	1028 ± 234	3.12 ± 0.81	4755 ± 1015	161 ± 18	0.9989 ± 0.0005	9.7 ± 0.8	148 ± 13	14.15
27℃	%06	1801 ± 211	0.31 ± 0.03	2941 ± 266	4.63 ± 0.57	35696 ± 2984	323 ± 18	0.9975 ± 0.0006	3.9 ± 0.2	139 ± 13	10.93
	100%	1086 ± 95	0.45 ± 0.02	2218 ± 191	4.79 ± 0.42	24903 ± 2091	273 ± 19	0.9988 ± 0.0002	4.9 ± 0.4	179 ± 12	5.73
	110%	1675 ± 214	0.36 ± 0.02	1592 ± 178	3.28 ± 0.19	11 944 ± 1844	217 ± 20	0.9991 ± 0.0003	5.8 ± 0.3	162 ± 11	10.33

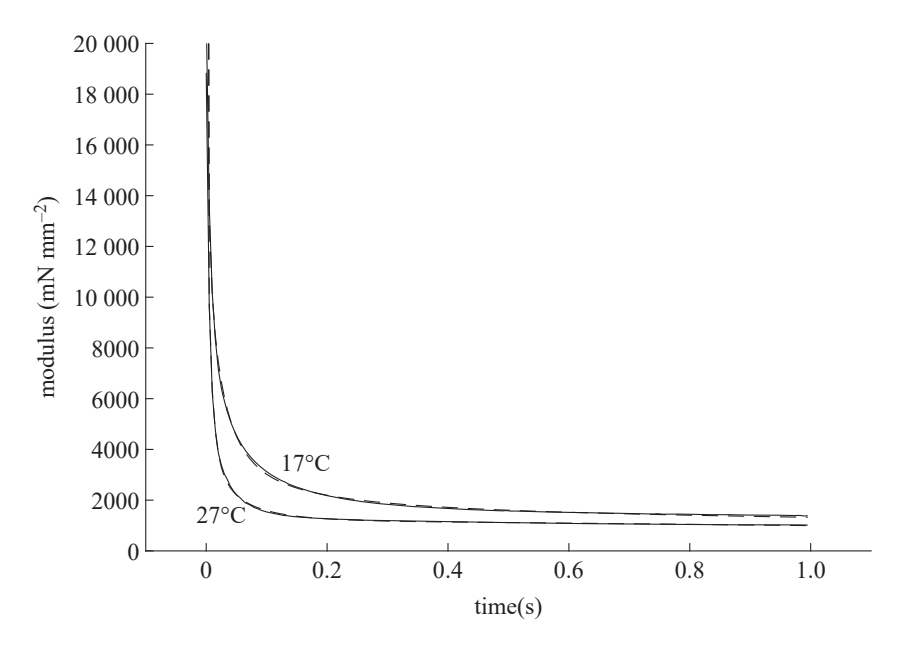


Figure 4. Temperature dependence of the modulus following a step-stretch. Solid black lines show the average modulus response plotted against time response at 17° C and 27° C. Temperature-dependent differences in cross-bridge cycling underlie the different dynamics shown between these two traces. Dashed lines represent fits of these average data to equation (2.2), with average parameter values from the fits listed in table 1. n = 10 muscles.

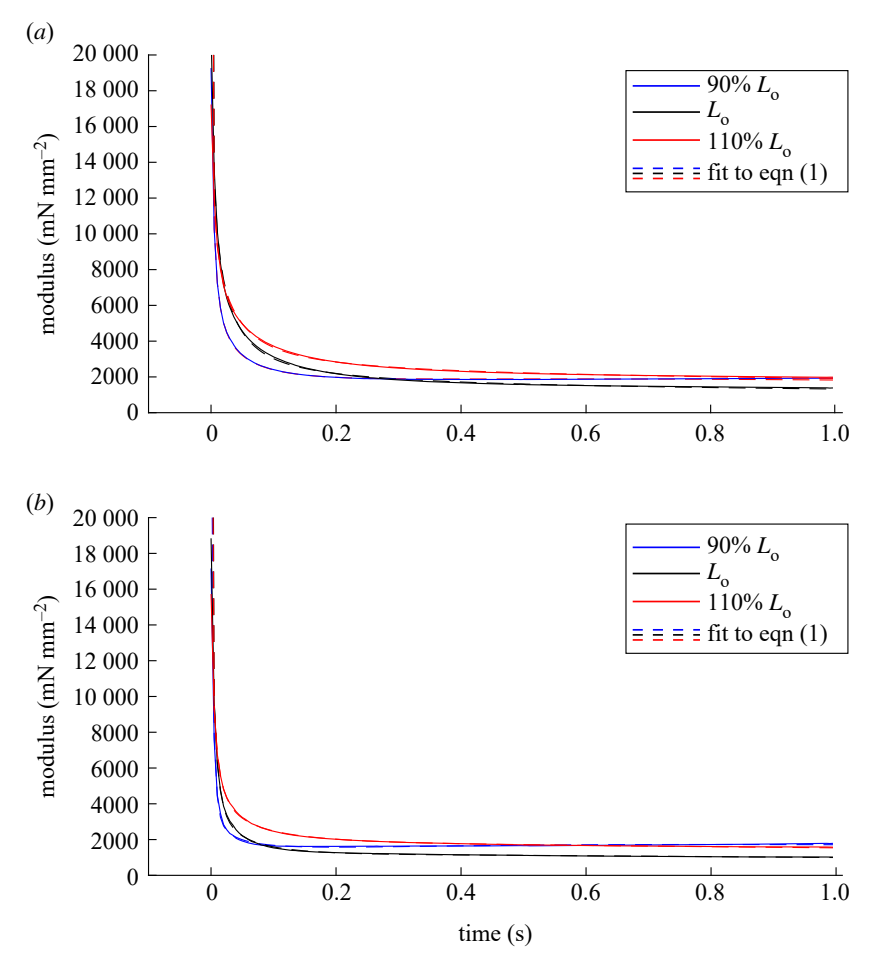


Figure 5. Effects of MTU length on modulus following a step-stretch at (a) 17° C and (b) 27° C. Solid lines show the average modulus response plotted against time for a given length, and dashed lines represent fits of these average data to equation (2.2). Length-dependent differences in cross-bridge cycling underlie the different dynamics shown by the blue, black and red traces within each panel. n = 10 muscles. (Online version in colour.)

B values were greatest at the shortest MTU lengths for both temperatures and decreased as the MTU length increased (with this effect of the length being more graded at 27°C), suggesting fewer cross-bridge recruitment events as the MTU length

increased. *B* values were slightly greater at 27°C versus 17°C, suggesting more cross-bridge recruitment events at the higher temperature. Values for the kinetics parameter representing cross-bridge recruitment, $2\pi b$, was not affected by

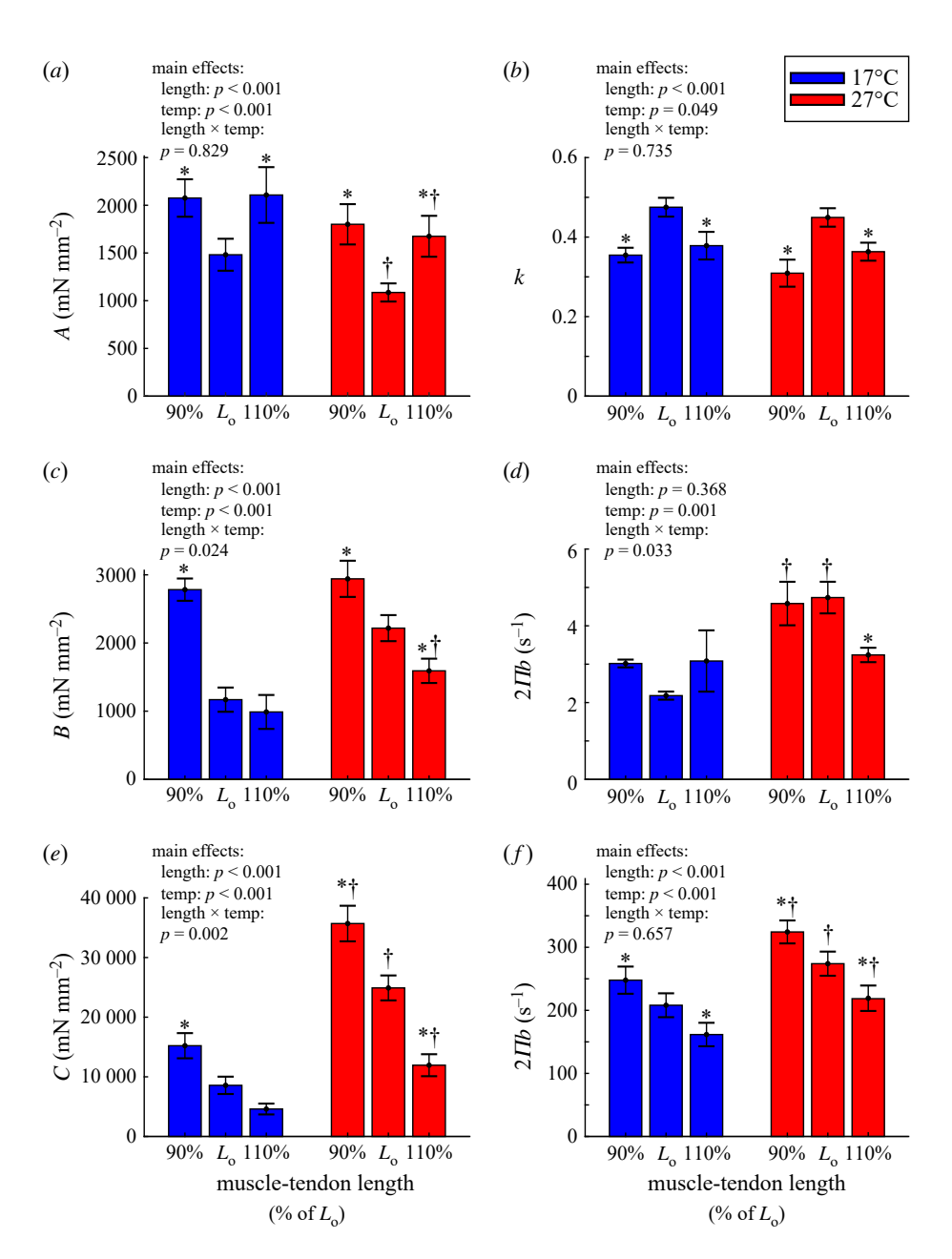


Figure 6. Moduli values were fitted to equation (2.2) to provide estimates of tissue viscoelasticity, cross-bridge binding and cross-bridge kinetics. (a,b) Parameter A represents the combined mechanical stress of the muscle, while parameter k describes the viscoelasticity of these passive elements (0 = purely elastic response, 1 = purely viscous response). (c,d) Parameter B represents the magnitude of work-producing muscle mechanics, with parameter $2\pi b$ representing the cross-bridge recruitment rate. (e,f) Parameter C represents the magnitude of work-absorbing muscle mechanics, with parameter $2\pi c$ representing the cross-bridge detachment rate. Asterisks denote differences from the measured value at L_0 within a temperature (p < 0.05), and daggers denote differences between temperatures for the same muscle length. n = 10 muscles.

changes in the muscle length. The $2\pi b$ values were greater at 27°C versus 17°C, suggesting faster cross-bridge recruitment kinetics at the higher temperature (figure 6d).

Downloaded from https://royalsocietypublishing.org/ on 12 May 202

C values were greatest at the shortest MTU length and decreased as the muscle length increased, and C values increased with the temperature (figure 6e), suggesting more cross-bridge detachment events in both cases. Values for the kinetics parameter $2\pi c$ were greatest at the shortest MTU length and decreased as the MTU length increased, suggesting that cross-bridge detachment slowed as the muscle length increased at both temperatures (figure 6f). The value of $2\pi c$ also increased at 27° C versus 17° C, suggesting that cross-bridge detachment was faster at the higher temperature. More specifically, $2\pi c$ was approximately 20% greater at 90% MTU length and approximately 21% smaller at 110% in

comparison to $L_{\rm o}$ values (at both temperatures), suggesting a 10% perturbation in the MTU length about $L_{\rm o}$ alters crossbridge detachment kinetics by 20% in mouse soleus muscles during tetanic contraction.

4. Discussion

We adapted step-stretch perturbation analysis methods to describe length-dependent cross-bridge kinetics in intact, isometrically contracting skeletal muscle during tetanus. We evaluated muscle function at two different temperatures (27°C versus 17°C) to demonstrate our capacity to detect expected increases in cross-bridge kinetics associated with established enzyme properties of myosin as an ATPase [35–38]. Many estimates of myosin Q_{10} values from solution

biochemistry experiments yield values of 2-3 [38-40] and clearly show that ATPase values increase with the temperature. We observed faster cross-bridge recruitment rates (Q₁₀ of 2.2 for $2\pi b$) and detachment rates (Q_{10} of 1.3 for $2\pi c$) as the temperature increased from 17°C to 27°C (figures 4 and 6). In concert with prior applications of this system analysis method to permeabilized muscle fibre preparations, we propose this represents a valid methodical framework to estimate the length-dependent cross-bridge activity during tetanic contraction. These whole-muscle Q_{10} estimates occur at the same order of magnitude as prior single-fibre assays, such as rabbit soleus fibres $(2\pi b \ Q_{10} = 7.3, 2\pi c \ Q_{10} = 3.6)$ [37]. Consistent with our findings, the rate of cross-bridge recruitment was more temperature sensitive than detachment [39,41].

Slower cross-bridge detachment rates have been observed at longer sarcomere lengths during isometric contractions in both permeabilized cardiomyocytes and skeletal fibres, including both fast and slow-twitch fibres [8,9,42-44]. In a previous study utilizing permeabilized rat soleus fibres, we observed a 15% slower rate of cross-bridge detachment when the sarcomere length was increased from 2.0 to 2.5 µm [8]. To test whether these length-dependent properties extended beyond single permeabilized cells to influence the behaviour of intact muscle in physiologically relevant manner, we applied step-perturbation analysis to estimate cross-bridge kinetics during isometric contractions in intact soleus as the MTU length changed $\pm 10\%$ from L_0 . We found that the rate of cross-bridge detachment was roughly 20% faster at the shorter muscle length and 20% slower at the longer muscle length compared to L_o , for both temperatures (figures 5 and 6). Therefore, the length-dependent slowing of cross-bridge kinetics at longer lengths appears to be conserved (or perhaps amplified) in intact, contracting soleus muscle. Our findings are consistent with a prior study showing that the rate of tension redevelopment (k_{TR}) was approximately 40% slower at Lo compared to 90% of L_o in intact rat cardiac trabeculae during isometric, tonic contractions (induced via K^+) [43]. In combination, these changes in length-dependent cross-bridge kinetics from various permeabilized muscle and intact muscle preparations suggest consistency among mechanosensitive properties of myosin cross-bridges that likely contribute to analogous characteristics of the whole-muscle function.

Downloaded from https://royalsocietypublishing.org/ on 12 May 202

We did not observe a significant length-dependent effect on the rate of cross-bridge recruitment $(2\pi b)$ in these intact soleus preparations (figure 6), nor in our previous permeabilized soleus fibre preparations [8]. However, McDonald et al. observed that following a rapid slack-stretch manoeuvre, the rate of tension redevelopment increased in permeabilized psoas fibres [45], suggesting that the rate of cross-bridge binding was accelerated. This finding would be in line with observations from a study by Wang et al., which showed approximately 15% increase in the rate of cross-bridge binding in rabbit psoas fibres when the sarcomere length was increased from 2.1 to 2.4 µm [42]. Conversely, Milani-Nejad et al. measured slower tension redevelopment at longer muscle length in intact cardiac trabeculae [43]. However, myosin detachment (not recruitment) is the rate-limiting step of the cross-bridge cycle in muscle fibres [41], and changes in the recruitment rate may have less impact on overall cycling behaviour than changes in the detachment rate. This is supported by our previous measurements in permeabilized fibre preparations as [MgATP] varied, showing that the cross-bridge detachment rate slowed as the sarcomere length increased due to slower rates of MgADP release from strongly bound cross-bridges [8,9].

Along with changes in cross-bridge kinetics, we also observed approximately 5-14% increase in tetanic, steadystate force following the 1% step-stretch (i.e. $\sigma_{\text{final}} > \sigma_0$; figure 3 and table 1). The increase in force at this slightly longer MTU length was greater than can be explained by any movement along the force-length curve, which would be less than approximately 2-3% increase on the ascending limb or any comparable decreases in force with the 1% length increase on the descending limb of the force-length curve (figure 2). Thus, the increases in σ_{final} from σ_0 likely reflect similarities to residual force enhancement although we did not perform any isometric at the 1% longer MTU length before the stepstretch to directly assess residual force enhancement as it is traditionally observed in single fibres [46,47].

Passive elements of the muscle also possess length-dependent properties that will influence their force contribution as the length of the muscle-tendon unit changes. Here, we must consider both the extracellular passive components, such as the aponeurosis and tendon, as well as the intracellular passive components, the most notable of these being titin. These elements primarily behave as non-linear elastic springs. Moreover, when the force decreases immediately after the step, the tendon will shorten and the muscle will lengthen because the MTU length is isometric. Therefore, the non-isometric conditions during this phase could lead to some force-velocity effects that are not accounted for by the analysis used. We do not think that this effect would change the main results for two reasons: (i) the velocity should be small because the length change in the tendon due to the step is relatively small and (ii) the effect would be consistent between conditions. Moreover, neither effect would change the statistical comparisons that were made.

Studies have also shown that titin in particular may have a direct role in modulating force during and after length changes imposed on striated muscle [48,49]. Titin PEVK regions may interact with the thin-filament during activation in a manner which decreases the spring length and increases titin stiffness, resulting in greater passive force during stretch. This phenomenon may contribute to our observations herein; for instance, we observed significantly larger A values during step-stretches which occurred at 90% $L_{\rm o}$ and at 110% $L_{\rm o}$ compared to the optimal muscle length (figure 6). This may be explained by increased short-range stiffness due to increased actin-titin interactions at the shorter MTU length.

We hypothesize that the changes in force distribution throughout the sarcomere, as it is stretched to longer lengths, could evoke strain-dependent changes in the MgADP release rate from strongly bound cross-bridges. Any increases in force that accompany increases in the muscle length (and sarcomere length) would be distributed throughout the sarcomere, myofilaments and bound cross-bridges [1,50,51]. Given that MgADP release depends on a conformational change that is coupled to the additional movement of the lever arm [52-54], then any increased load borne by a bound cross-bridge would impede MgADP dissociation and slow the rate of cross-bridge detachment [8,9]. Our findings suggest that these load-dependent pathways are preserved in the whole skeletal muscle as the length changes (statically), which could intrinsically modulate the energetics

An understanding of how muscle contracts and responds to physiological demands requires an assessment of the effects of changes in muscle length on kinetic and energetic aspects of force production. Our new findings help to extend our understanding of length-dependent cross-bridge activity from the fibre into the whole-muscle-tendon unit. Summary data imply that that cross-bridge cycling kinetics are mediated by length-dependent properties, such as strain-dependent MgADP release, to impact how chemical energy is used to produced force. This mechanism may serve to enhance the efficiency of energy utilization at longer muscle lengths by prolonging the time myosin spend in the strongly bound, force-generating phase of the cross-bridge cycle and serve as a length-dependent mechanism that modulates myosin efficiency throughout muscle contraction.

Ethics. All procedures were approved by the Institutional Animal Care and Use Committee at Washington State University and complied with the Guide for the Use and Care of Laboratory Animals published by the National Institutes of Health. Male C57BL/6 mice (7 weeks old) were sourced from Simonsen Laboratories. Ten mice were anaesthetized by isoflurane inhalation (3% volume in 95% O₂-5% CO₂ flowing at 2 l min⁻¹), then a soleus muscle was removed, preserving as much of the proximal and distal tendons as possible.

Data accessibility. Datasets for the experiments reported in this paper are available from the Dryad Data Repository at https://doi.org/10. 5061/dryad.tb2rbnzx8 [55].

Authors' contributions. A.J.F.: conceptualization, data curation, formal analysis, investigation, methodology, visualization, writing—original draft, writing-review and editing; D.C.L.: conceptualization, methodology, resources, validation, writing-review and editing; B.C.W.T.: conceptualization, funding acquisition, investigation, methodology, project administration, resources, software, supervision, validation, writing—review and editing.

All authors gave final approval for publication and agreed to be held accountable for the work performed therein.

Competing interests. We declare we have no competing interests. Funding. This work was supported by the National Science Foundation (1656450 to B.C.W.T.), American Heart Association (19TPA34860008 to B.C.W.T.), National Institutes of Health (R01 HL149164 to B.C.W.T.) and the Army Research Office (ARO 66554-EG to D.C.L.). Acknowledgements. We thank Dr James Peters and Dr Anita Vasavada for suggestions on this manuscript, and Dave Savage for his assistance designing and building components.

References

Downloaded from https://royalsocietypublishing.org/ on 12 May 202

- Horowits R, Podolsky RJ, Horrowits R, Podolsky RJ. 1987 The positional stability of thick filaments in activated skeletal muscle depends on sarcomere length: evidence for the role of titin filaments. J. Cell Biol. 105, 2217-2223. (doi:10.1083/jcb.105.5. 2217)
- 2. Linke WA. 2008 Sense and stretchability: the role of titin and titin-associated proteins in myocardial stress-sensing and mechanical dysfunction. Cardiovasc. Res. 77, 637-648. (doi:10.1016/j. cardiores.2007.03.029)
- Linari M, Brunello E, Reconditi M, Fusi L, Caremani M, Narayanan T, Piazzesi G, Lombardi V, Irving M. 2015 Force generation by skeletal muscle is controlled by mechanosensing in myosin filaments. Nature 528, 276-279. (doi:10.1038/ nature15727)
- Allen JD, Moss RL. 1987 Factors influencing the ascending limb of the sarcomere length-tension relationship in rabbit skinned muscle fibres. J. Physiol. 390, 119-136. (doi:10.1113/jphysiol. 1987.sp016689)
- Konhilas JP, Irving TC, de Tombe PP. 2002 Lengthdependent activation in three striated muscle types of the rat. J. Physiol. 544, 225-236. (doi:10.1113/ jphysiol.2002.024505)
- ter Keurs HE, Iwazumi T, Pollack GH. 1978 The sarcomere length-tension relation in skeletal muscle. J. Gen. Physiol. 72, 565-592. (doi:10.1085/ jqp.72.4.565)
- Stephenson DG, Williams DA. 1982 Effects of sarcomere length on the force-pCa relation in fastand slow-twitch skinned muscle fibres from the rat. J. Physiol. 333, 637-653.

- Fenwick AJ, Leighton SR, Tanner BCW. 2016 Myosin MgADP release rate decreases as sarcomere length increases in skinned rat soleus muscle fibers. Biophys. *J.* **111**, 2011–2023. (doi:10.1016/j.bpj.2016.09.024)
- Tanner BCW, Breithaupt JJ, Awinda PO. 2015 Myosin MgADP release rate decreases at longer sarcomere length to prolong myosin attachment time in skinned rat myocardium. Am. J. Physiol.—Hear. Circ. Physiol. 309, H2087-H2097. (doi:10.1152/ ajpheart.00555.2015)
- 10. Stehle R, Brenner B. 2000 Cross-bridge attachment during high-speed active shortening of skinned fibers of the rabbit psoas muscle: implications for cross-bridge action during maximum velocity of filament sliding. Biophys. J. 78, 1458-1473. (doi:10. 1016/S0006-3495(00)76699-9)
- 11. Fenwick AJ, Wood AM, Tanner BCW. 2017 Effects of cross-bridge compliance on the force-velocity relationship and muscle power output. PLoS One 12, e0190335. (doi:10.1371/journal.pone.0190335)
- 12. Fenn WO. 1924 The relation between the work performed and the energy liberated in muscular contraction. J. Physiol. 58, 373-395. (doi:10.1113/ jphysiol.1924.sp002141)
- 13. Kawai M, Brandt PW. 1980 Sinusoidal analysis: a high resolution method for correlating biochemical reactions with physiological processes in activated skeletal muscles of rabbit, frog and crayfish. J. Muscle Res. Cell Motil. 1, 279-303. (doi:10.1007/BF00711932)
- 14. Campbell KB, Chandra M, Kirkpatrick RD, Slinker BK, Hunter WC. 2004 Interpreting cardiac muscle forcelength dynamics using a novel functional model. Am J Physiol Hear. Circ Physiol. 286, H1535-H1545. (doi:10.1152/ajpheart.01029.2003)

- 15. Palmer BM, Suzuki T, Wang Y, Barnes WD, Miller MS, Maughan DW. 2007 Two-state model of actomyosin attachment-detachment predicts C-process of sinusoidal analysis. Biophys. J. 93, 760-769. (doi:10.1529/biophysj.106.101626)
- 16. Civan MM, Podolsky RJ. 1966 Contraction kinetics of striated muscle fibres following quick changes in load. J. Physiol. 184, 511-534. (doi:10.1113/ jphysiol.1966.sp007929)
- 17. Huxley AF, Simmons RM. 1971 Proposed mechanism of force generation in striated muscle. Nature 233, 533-538. (doi:10.1038/233533a0)
- Pringle JWS. 1978 Stretch activation of muscle: function and mechanism. Proc. R. Soc. Lond. B 201, 107-130. (doi:10.1098/rspb.1978.0035)
- 19. Ford LE, Huxley AF, Simmons RM. 1977 Tension responses to sudden length change in stimulated frog muscle fibres near slack length. J. Physiol. 269, 441-515. (doi:10.1113/jphysiol.1977.
- 20. Davis JS, Rodgers ME. 1995 Force generation and temperature-jump and length-jump tension transients in muscle fibers. Biophys. J. 68, 2032-2040. (doi:10.1016/S0006-3495(95)80380-2)
- 21. Barton ER, Lynch G. 2008 Measuring isometric force of isolated mouse muscles in vitro. See https://treatnmd.org/wp-content/uploads/2016/08/cmd-DMD M.1.002.pdf.
- 22. Mohammed GA, Hou M. 2016 Optimization of active muscle force-length models using least squares curve fitting. IEEE Trans. Biomed. Eng. 63, 630-635. (doi:10.1109/TBME.2015.2467169)
- 23. Sacks RD, Roy RR. 1982 Architecture of the hind limb muscles of cats: functional significance.

- *J. Morphol.* **173**, 185–195. (doi:10.1002/jmor. 1051730206)
- Burkholder TJ, Fingado B, Baron S, Lieber RL. 1994
 Relationship between muscle fiber types and sizes
 and muscle architectural properties in the mouse
 hindlimb. *J. Morphol.* 221, 177–190. (doi:10.1002/jmor.1052210207)
- Brooks SV, Faulkner JA 1988 Contractile properties of skeletal muscles from young, adult and aged mice. J. Physiol. 404, 71–82. (doi:10.1113/jphysiol. 1988.sp017279)
- Mendez J, Keys A. 1960 Density and composition of mammalian muscle. *Metabolism* 9, 184–188.
- Huxley AF. 1974 Muscular contraction. J. Physiol. 243, 1–43.
- Tanner BCW, Wang Y, Maughan DW, Palmer BM.
 2011 Measuring myosin cross-bridge attachment time in activated muscle fibers using stochastic vs. sinusoidal length perturbation analysis. *J. Appl. Physiol.* 110, 1101–1108. (doi:10.1152/japplphysiol. 00800.2010)
- Palmer BM, Tanner BCW, Toth MJ, Miller MS. 2013
 An inverse power-law distribution of molecular bond lifetimes predicts fractional derivative viscoelasticity in biological tissue. *Biophys. J.* 104, 2540–2552. (doi:10.1016/j.bpj.2013.04.045)
- Kawai M, Wray JS, Zhao Y. 1993 The effect of lattice spacing change on cross-bridge kinetics in chemically skinned rabbit psoas muscle fibers. I: proportionality between the lattice spacing and the fiber width. *Biophys. J.* 64, 187–196. (doi:10.1016/ S0006-3495(93)81356-0)
- Kawai M, Halvorson HR. 1991 Two step mechanism of phosphate release and the mechanism of force generation in chemically skinned fibers of rabbit psoas muscle. *Biophys. J.* 59, 329–342. (doi:10. 1016/S0006-3495(91)82227-5)

Downloaded from https://royalsocietypublishing.org/ on 12 May 202

- Cui L, Perreault EJ, Maas H, Sandercock TG. 2008 Modeling short-range stiffness of feline lower hindlimb muscles. *J. Biomech.* 41, 1945–1952. (doi:10.1016/j.jbiomech.2008.03.024)
- Rigozzi S, Müller R, Snedeker JG. 2009 Local strain measurement reveals a varied regional dependence of tensile tendon mechanics on glycosaminoglycan content. J. Biomech. 42, 1547–1552. (doi:10.1016/j. jbiomech.2009.03.031)
- Rehwaldt JD, Rodgers BD, Lin DC. 2017 Skeletal muscle contractile properties in a novel murine model for limb girdle muscular dystrophy 2i.

- *J. Appl. Physiol.* **123**, 1698–1707. (doi:10.1152/japplphysiol.00744.2016)
- Stein RB, Gordon T, Shriver J. 1982 Temperature dependence of mammalian muscle contractions and ATPase activities. *Biophys. J.* 40, 97–107. (doi:10. 1016/S0006-3495(82)84464-0)
- Zhao Y, Kawai M. 1994 Kinetic and thermodynamic studies of the cross-bridge cycle in rabbit psoas muscle fibers. *Biophys. J.* 67, 1655–1668. (doi:10. 1016/S0006-3495(94)80638-1)
- Wang G-Y, Kawai M. 2001 Effect of temperature on elementary steps of the cross-bridge cycle in rabbit soleus slow-twitch muscle fibres. *J. Physiol.* 531, 219–234. (doi:10.1111/j.1469-7793.2001.0219j.x)
- Stienen GJ, Kiers JL, Bottinelli R, Reggiani C. 1996 Myofibrillar ATPase activity in skinned human skeletal muscle fibres: fibre type and temperature dependence. *J. Physiol.* 493(Pt 2), 299–307. (doi:10.1113/jphysiol.1996.sp021384)
- Ranatunga KW. 2018 Temperature effects on force and actin-myosin interaction in muscle: a look back on some experimental findings. *Int. J. Mol. Sci.* 19, 1538. (doi:10.3390/ijms19051538)
- He ZH, Bottinelli R, Pellegrino MA, Ferenczi MA, Reggiani C. 2000 ATP consumption and efficiency of human single muscle fibers with different myosin isoform composition. *Biophys. J.* 79, 945–961. (doi:10.1016/S0006-3495(00)76349-1)
- Siemankowski RF, Wiseman MO, White HD. 1985
 ADP dissociation from actomyosin subfragment 1 is sufficiently slow to limit the unloaded shortening velocity in vertebrate muscle. *Proc. Natl. Acad. Sci. USA* 82, 658–662. (doi:10.1073/pnas.82.3.658)
- 42. Wang G-Y, Ding W, Kawai M. 1999 Does thin filament compliance diminish the cross-bridge kinetics? A study in rabbit psoas fibers. *Biophys. J.* **76**, 978–984. (doi:10.1016/S0006-3495(99) 77261-9)
- Milani-Nejad N, Xu Y, Davis JP, Campbell KS, Janssen PML. 2013 Effect of muscle length on crossbridge kinetics in intact cardiac trabeculae at body temperature. J. Gen. Physiol. 141, 133–139. (doi:10. 1085/jgp.201210894)
- Pulcastro HC, Awinda PO, Breithaupt JJ, Tanner BCW. 2015 Effects of myosin light chain phosphorylation on length-dependent myosin kinetics in skinned rat myocardium. Arch. Biochem. Biophys. 601, 56–68. (doi:10.1016/j.abb. 2015.12.014)

- McDonald KS, Wolff MR, Moss RL. 1997 Sarcomere length dependence of the rate of tension redevelopment and submaximal tension in rat and rabbit skinned skeletal muscle fibres. *J. Physiol.* 501(Pt 3), 607–621. (doi:10.1111/j.1469-7793.1997.607bm.x)
- Leonard TR, DuVall M, Herzog W. 2010 Force enhancement following stretch in a single sarcomere. Am. J. Physiol. Cell Physiol. 299, C1398—C1401. (doi:10.1152/ajpcell.00222.2010)
- Edman KAP, Elzinga G, Noble MIM. 1982 Residual force enhancement after stretch of contracting frog single muscle fibers. *J. Gen. Physiol.* 80, 769–784. (doi:10.1085/jgp.80.5.769)
- Nishikawa KC, Monroy JA, Uyeno TE, Yeo SH, Pai DK, Lindstedt SL. 2012 Is titin a 'winding filament'? A new twist on muscle contraction. *Proc. R. Soc. B* 279, 981–990. (doi:10.1098/rspb.2011.1304)
- Rode C, Siebert T, Blickhan R. 2009 Titin-induced force enhancement and force depression: a 'stickyspring' mechanism in muscle contractions? *J. Theor. Biol.* 259, 350–360. (doi:10.1016/j.jtbi.2009.03.015)
- Huxley HE, Stewart A, Sosa H, Irving TC. 1994 X-ray diffraction measurements of the extensibility of actin and myosin filaments in contracting muscle. *Biophys. J.* 67, 2411–2421. (doi:10.1016/S0006-3495(94)80728-3)
- Wakabayashi K, Sugimoto Y, Tanaka H, Ueno Y, Takezawa Y, Amemiya Y. 1994 X-ray diffraction evidence for the extensibility of actin and myosin filaments during muscle contraction. *Biophys. J.* 67, 2422–2435. (doi:10.1016/S0006-3495(94) 80729-5)
- Capitanio M, Canepari M, Cacciafesta P, Lombardi V, Cicchi R, Maffei M, Pavone FS, Bottinelli R. 2006 Two independent mechanical events in the interaction cycle of skeletal muscle myosin with actin. *Proc. Natl. Acad. Sci. USA* 103, 87–92. (doi:10. 1073/pnas.0506830102)
- Smith DA, Geeves MA. 1995 Strain-dependent crossbridge cycle for muscle. *Biophys. J.* 69, 524–537. (doi:10.1016/S0006-3495(95)79926-X)
- Nyitrai M, Geeves MA. 2004 Adenosine diphosphate and strain sensitivity in myosin motors. *Philos. Trans. R Soc. L. B Biol. Sci.* 359, 1867–1877. (doi:10. 1098/rstb.2004.1560)
- Fenwick AJ, Lin DC, Tanner BCW. 2021 Data from: Myosin cross-bridge kinetics slow at longer muscle lengths during isometric contractions in intact soleus from mice. Dryad Digital Repository. (doi:10. 5061/dryad.tb2rbnzx8)